



## Semester Project Proposal

Development of a Model Predictive Controller for  
FALCON: Fixed-wing Aerial Lifting and Carrying  
of Objects inspired by Nature

Aurel X. Appius

September 2022

Supervision

Yasunori Toshimitsu  
Prof. Dr. Robert K. Katzschmann

### Abstract

Aerial grasping of objects is a problem, where nature is still miles ahead of robotics. When comparing an eagle grasping a fish out of the water with a modern grasping robot, the difference in agility, speed and precision is clearly notable. The pick-up speed, the grasping success rate as well as the ability to cope with disturbances caused by the environment are some examples of current animal superiority over robots. To bring robots one step closer to its natural counterpart, we want to autonomously grasp an object using a fixed wing aircraft. To achieve this, we want to use a model predictive controller on a lightweight model plane equipped with a soft robotic gripper. A coordinated movement between the plane and the gripper, should decrease the relative speed of the gripper to the object, resulting in a high gripping success rate. By using a fixed wing aircraft, we can perform the pick-up more energy efficiently than quadcopters and therefore stay in the air for longer time periods. Furthermore, fixed-wing aircraft have less downwash than quadcopters, allowing them to also pick-up lightweight objects, that would blow away in a quadcopter pick-up scenario.

## Contents

<b>1</b>	<b>Introduction</b>	<b>1</b>
1.1	Motivation . . . . .	1
1.2	Related Work . . . . .	1
<b>2</b>	<b>Goals and Deliverables</b>	<b>2</b>
<b>3</b>	<b>Methodology</b>	<b>2</b>
3.1	Grasp Plan . . . . .	2
3.2	Flight Plan . . . . .	2
3.3	Modeling and Control . . . . .	3
3.3.1	Gripper Dynamics . . . . .	3
3.3.2	Plane Dynamics . . . . .	4
3.3.3	Plane Actuators . . . . .	4
3.3.4	Determining the Moment of Inertia . . . . .	5
3.3.5	Fixed-Wing Aerodynamics . . . . .	6
3.3.6	Control Approach . . . . .	8
3.3.7	Model Predictive Plane Controller . . . . .	9
3.4	Controller Architecture . . . . .	10
3.5	System Architecture . . . . .	11
3.6	Timeline . . . . .	12
<b>4</b>	<b>Future Work</b>	<b>12</b>

# 1 Introduction

## 1.1 Motivation

Roboticians throughout history have always looked to nature when faced with difficult problems. Through thousand years of evolution, animals became very skilled and efficient in performing difficult dynamic maneuvers. A very impressive feat is the grasping ability of predatory birds, who can pick up objects from the ground in a dynamic swooping motion. Fast maneuvers like these, require both high precision and an agile body. Figure 1 shows a sequence of a bald eagle, that performs a grasping maneuver. When looking at the sequence, we observe that the eagle approaches the fish with his claws in the front. During the pick-up his body moves over the fish, while the claws perform a backwards motion to compensate for the forward speed. When the eagle finishes the grasping maneuver, the claws are in the back. A robot that could achieve similar performance would be of great interest for both industry and research.



Figure 1: An Eagle grasping a fresh salmon from the end of a boat. Still images taken from a video found in New York Post (2017).

## 1.2 Related Work

Various researchers have already tried to do grasping of objects in an eagle like manner. The most common approach is the combination of a gripper with a quadcopter. Gawel et al. (2017) used a magnetic gripper to pick up ferrous objects while moving. Fiaz et al. (2018) combined a permanent magnetic gripper with a dropping mechanism to let go of objects on demand. Roderick et al. (2021) achieved a very bio-like perching of branches by using a combination of an arm and a gripper. Generally said, there has been many works on quadcopter based aerial grasping and perching.

Hingston et al. (2020) designed a net- and a slider-based gripper for aerial grasping with quadcopters. Another gripper mechanism for quad-rotors by Zhang et al. (2019) was used for perching onto power lines to recharge the battery. Another interesting design by McLaren et al. (2019) uses passive gripper to achieve very fast grasping speeds.

All the mentioned robots that can perform grasps and perches are quad-rotors. They have the ability to hover and can temporarily halt during a grasping maneuver. There are some quadcopters that can grasp without stopping over the object (Appius et al., 2022), (Fishman et al., 2021), (Thomas et al., 2014). This allows a fast pickup but requires a lot of energy. Fixed-wing aircraft outperform quadcopters drastically when it comes to specific energy consumption as well as energy per distance (Karydis & Kumar, 2017). An eagle can both grasp an object dynamically and then fly long distances without needing a recharge every 10 minutes.

Another issue with quadcopter grasping is the downwash of the rotors (Zhu et al., 2022). The high winds caused by the propellers can blow away the object that the quadcopter wanted to grasp making the task nearly impossible. This effect becomes particularly noticeable when picking up lightweight objects.

Stewart et al. (2022) used a fixed-wing aircraft in combination with a passive gripper to grasp objects dynamically. They achieved grasping speeds of 8 m/s, but due to the passive gripper the robot can't drop the object and is therefore limited. The rigid gripper is also limited in grasping fragile or delicate objects, due to its rigid nature.

Moreover the system proposed by Stewart et al. (2022) is not fully autonomous and relies on a human pilot to fly. They could only demonstrate a single successful aerial grasp.

A review paper by Meng et al. (2021) summarized the current state of aerial grasping robots. According to

Meng et al. (2021) and my knowledge, a fully autonomous pick-up of objects using a fixed-wing aircraft has yet to be achieved.

## 2 Goals and Deliverables

I propose FALCON: Fixed-wing Aerial Lifting and Carrying of Objects inspired by Nature. A fixed-wing aerial robot, that is equipped with a soft robotic gripper. Using a model predictive controller, it should be able to grasp static objects off the ground autonomously.

The robot should be able to achieve the following goals:

**Grasping** Using a soft robotic gripper, FALCON should be able to grasp objects of different sizes and geometries consistently.

**Autonomy** FALCON should perform the whole flight and grasping maneuver fully autonomous.

## 3 Methodology

### 3.1 Grasp Plan

To account for the fast speeds during the grasping maneuver, the gripper will be placed on an arm. The idea is that the arm can move back while the aircraft passes over the object which results in a lower relative speed between the object and the gripper. This is exactly the movement, that we could observe for the eagles' pick-up of a fish in figure 1. This kind of motion gives the gripper more time to close and a successful pickup is likelier. An illustration of the principle can be seen in figure 2.

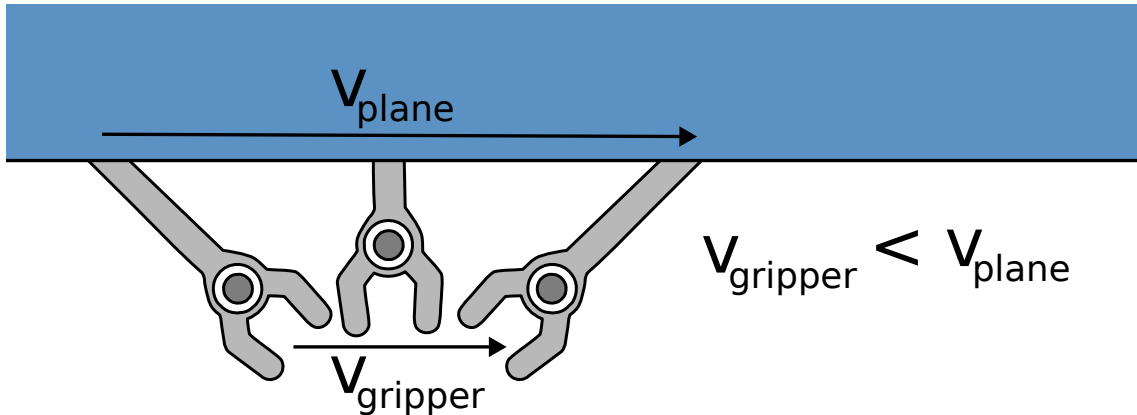


Figure 2: If the arm of the gripper rotates during the grasping sequence, the relative speed of the gripper is lower than the speed of the plane.

### 3.2 Flight Plan

The fixed-wing aircraft cannot hover like a quadcopter, so there needs to be a defined trajectory before and after the grasp. The simplest solution is to fly circuits over the target, which can be seen as the blue path in figure 3. Once the grasping sequence is initiated, the aircraft will change its trajectory and will perform a swooping motion which can be seen as the red path in figure 3. This is a pretty common practice for manned airplanes when approaching an airport and trying to land. If the landing maneuver fails, the plane ascends again and continues to fly a circuit above the runway to then retry the landing. Note that predatory birds also use this tactic when hunting for rodents on the ground.

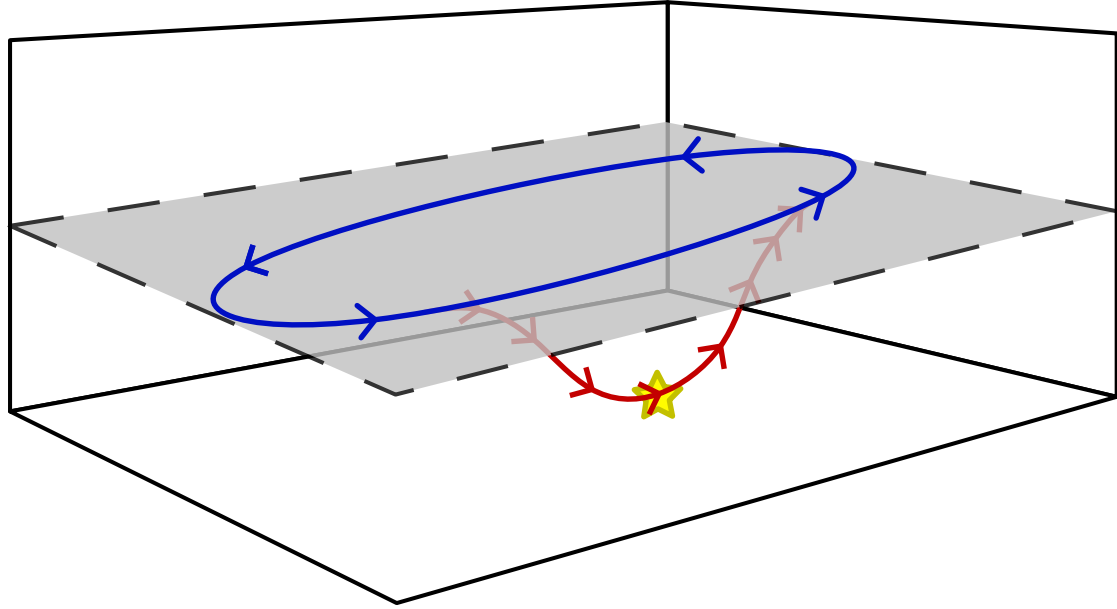


Figure 3: This sketch shows the planned flight path for the aircraft when grasping an object.

### 3.3 Modeling and Control

#### 3.3.1 Gripper Dynamics

The gripper is modeled as a point mass on an arm that is attached to the aircraft. The input  $u_{arm}$  controls the angle  $\beta$  of the gripper arm by applying a torque. For the controller described in section 3.3.7, the speed of the gripper is of great importance. By using the velocity transfer formula seen in equation 1, we can derive the grippers speed as a function of the planes speed  $v_{plane}$  and the angular velocity  $\dot{\beta}$ .

$$\vec{v}_{grip} = \vec{v}_{plane} + \dot{\beta} \times \vec{r}_{plane-grip} \quad (1)$$

Finally, we can derive the state space representation of the gripper dynamics, which can be seen in equation 2. After the grasping maneuver, the point mass at the end of the stick  $m_{gripper}$  will increase by the mass  $m_{obj}$ .

$$\frac{d}{dt} \begin{bmatrix} \beta \\ \dot{\beta} \end{bmatrix} = \begin{bmatrix} \dot{\beta} \\ \frac{\cos(\beta) \cdot g}{m_{gripper} \cdot l_{arm}} \end{bmatrix} + \begin{bmatrix} 0 \\ \frac{1}{m_{gripper} \cdot l_{arm}^2} \end{bmatrix} \cdot u_{arm} \quad (2)$$

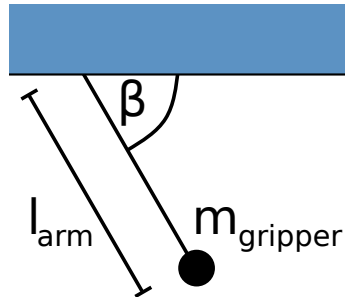


Figure 4: This sketch shows the proposed mathematical model for the gripper.

### 3.3.2 Plane Dynamics

To properly control the motion of the aircraft, a mathematical model of the plane's dynamics has to be derived. For this let us first define the coordinates of the plane. We do this by having an inertial frame and a body frame that is fixed to the aircraft. We denote the position of the aircraft with the vector  $\vec{X}_{plane}$ . As shown by Noth et al. (2006), the equations of motion can be derived by using the Lagrange-Euler approach. The Lagrangian is defined as seen in equation 3 where  $T$  denotes the kinetic and  $V$  denotes the potential energy.

$$\mathcal{L} = T - V \quad (3)$$

The equations of motion are found by inserting the Lagrangian into the differential equation seen in equation 4, where  $q$  denotes the generalized coordinates and  $\Gamma$  denotes the non-conservative forces. In our case the non-conservative forces come from the aerodynamic interactions of the plane with the environment.

$$\Gamma_i = \frac{d}{dt} \left( \frac{\partial \mathcal{L}}{\partial \dot{q}_i} \right) - \frac{\partial \mathcal{L}}{\partial q_i} \quad (4)$$

When solving and simplifying equation 4 for all state space coordinates  $q_i$ , which are defined in table 1, the state space dynamics of the plane are found. The final equations can be seen in equation 5.

Variable	Description	Variable	Description
$\phi$	Roll Angle	$x$	x-position
$\alpha$	Pitch Angle	$y$	y-position
$\psi$	Yaw Angle	$z$	z-position
$\dot{\phi}$	Roll Rate	$\dot{x}$	x-velocity
$\dot{\alpha}$	Pitch Rate	$\dot{y}$	y-velocity
$\dot{\psi}$	Yaw Rate	$\dot{z}$	z-velocity

Table 1: State space variables of the plane's dynamics

In the equations of motion seen in equation 5, gravity and aerodynamic forces are summed up as a force and a torque on the center of mass of the plane. A detailed derivation of these forces can be found in section 3.3.5.

$$\begin{aligned} \ddot{x} &= \frac{F_{tot,x}}{m} \\ \ddot{y} &= \frac{F_{tot,y}}{m} \\ \ddot{z} &= \frac{F_{tot,z}}{m} \\ \ddot{\phi} &= \frac{I_{pitch} - I_{yaw}}{I_{roll}} \dot{\psi} \dot{\alpha} + \frac{M_{tot,x}}{I_{roll}} \\ \ddot{\alpha} &= \frac{I_{yaw} - I_{roll}}{I_{pitch}} \dot{\psi} \dot{\phi} + \frac{M_{tot,y}}{I_{pitch}} \\ \ddot{\psi} &= \frac{I_{roll} - I_{pitch}}{I_{yaw}} \dot{\alpha} \dot{\phi} + \frac{M_{tot,z}}{I_{yaw}} \end{aligned} \quad (5)$$

### 3.3.3 Plane Actuators

A fixed-wing aircraft has four main actuators, that it can use to control its flight:

**The Propeller** is used to accelerate the plane in the x-direction of the body frame.

**The Ailerons** are used to control the aircraft's roll.

**The Rudder** is used to control the yaw of the plane.

**The Elevator** can change the pitch of the aircraft.

Figure 5 shows the four actuators, the body coordinate frame and the names of the rotations around each axis. Of course the actuation of a single actuator does not only result in the desired change of attitude, but also has some adverse effects. For example, a generally known effect is that the use of the ailerons results not only in a change of the roll angle but also a change in the yaw. Skilled pilots as well as control systems automatically compensate for that while flying.

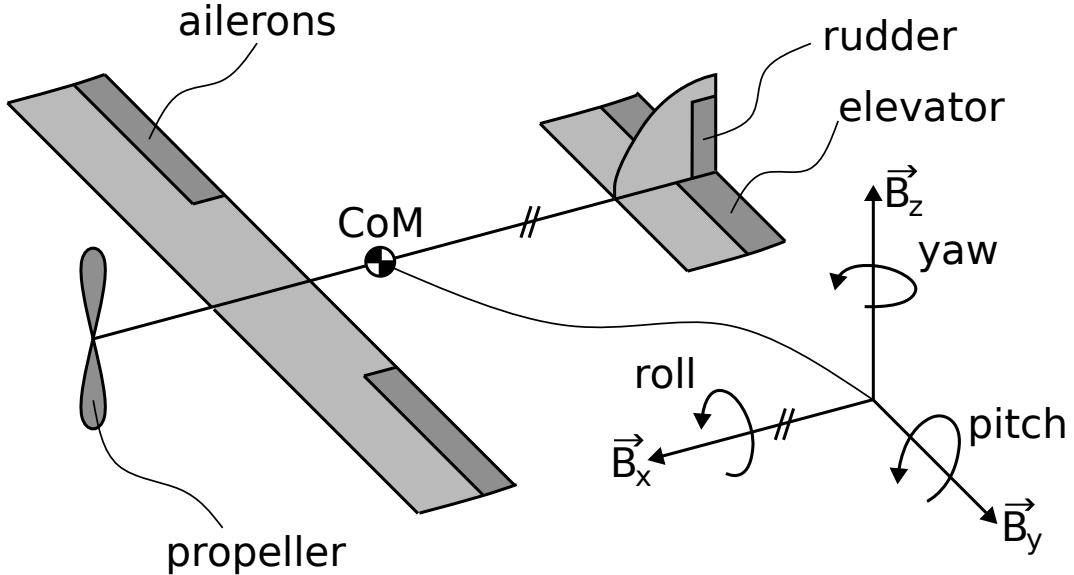


Figure 5: This sketch shows the simplified plane with all the parts that are important when mathematically modeling the plane as a dynamical system.

### 3.3.4 Determining the Moment of Inertia

The equations of motion seen in equation 5 are dependent on the moment of inertia  $I_x$ ,  $I_y$  and  $I_z$ . To use the model in a control algorithm, these values need to be determined. Koken (2017) proposes a simple but precise method to experimentally determine the moment of inertia of a model plane. The method works by letting the plane oscillate around a certain axis and then measuring the oscillation period  $T$ . The moment of inertia is then estimated using equation 6. The experimental setup to determine the inertia around each axis can be seen in figure 6.

$$I = \frac{m \cdot g \cdot D \cdot T^2}{16 \cdot \pi^2 \cdot h} \quad (6)$$

To verify the accuracy of the experiment, the same procedure is first done with an object where the moments of inertia are known or calculated analytically. The period length can be measured very accurately by using the flight controller IMU which has a gyroscope. To account for the mass of the gripper, we can correct the moment of inertia with an additional term as seen in equation 7. This correction formulation assumes that the gripper arm is attached to the origin of the plane, which is probably not true. In that case the moment can easily be adjusted with a constant offset term, which is found using the parallel axis theorem.

$$\begin{aligned} I_{pitch,corrected} &= I_{pitch} + m_{gripper}(l_{arm} \sin \beta)^2 \\ I_{yaw,corrected} &= I_{yaw} + m_{gripper}(l_{arm} \cos \beta)^2 \end{aligned} \quad (7)$$

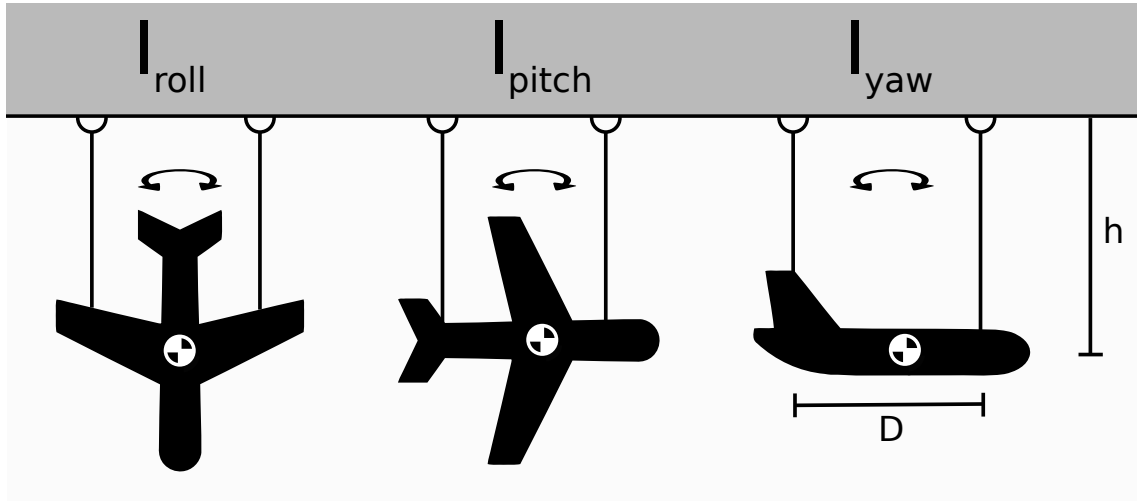


Figure 6: The orientation of hanging the plane to determine the moment of inertia experimentally by measuring the oscillation Time  $T$ .

### 3.3.5 Fixed-Wing Aerodynamics

In order to find a full mathematical representation of the system, the dynamic response of the control inputs need to be studied thoroughly. All controllable inputs can be seen in table 2. Only the inputs  $u_1$  to  $u_5$  are used to control the plane's flightpath.

Input Variable	Description	Unit
$u_1$	Motor Thrust	Newton
$u_2$	Left Aileron	Radian
$u_3$	Right Aileron	Radian
$u_4$	Elevator	Radian
$u_5$	Rudder	Radian
$u_{arm}$	Gripper Arm Angle	Radian
$u_{grip}$	Gripper Open/Close	[ $-$ ]

Table 2: Inputs of the system.

To control the aircraft, we need a model that is as simple as possible, but rich enough to describe the dynamics of the plane. I propose a model that can be seen in Fig. 7. The lift and drag of the airplane are determined experimentally. They are a function of the pitch of the aircraft as well as the speed at which it travels. Additionally, the control surfaces have an impact on the flight behavior, which are modeled by doing a conservation of momentum. The following List discusses the relation between the control inputs and the forces acting on the plane. The idea behind the modeling is to model the aircraft as an airfoil and the control inputs as perturbations. All forces seen in figure 7 are discussed in the following.

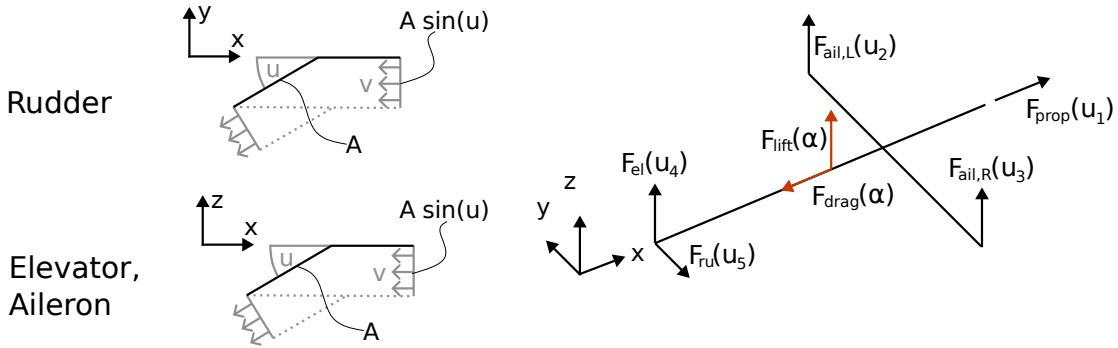


Figure 7: A simple model of an aircraft and figures clarifying the derivations in equations 8, 9 and 10.

**Rudder** The rudder is displacing air at the end of the airplane. We can model the force that this causes on the tail of the airplane by just comparing the incoming and outgoing momentum of the air affected by the deflection of the tail. In equation 8,  $A_5$  refers to the area of the rudder and  $v$  to the speed of the plane. If we assume that  $u_5$  is a small angle, we can use the first order Taylor approximation of the sine and cosine to further simplify the expression. This gives us a good estimate of the force caused by deflection of the rudder.

$$\begin{aligned} \left[ \begin{array}{c} F_x \\ F_y \\ F_z \end{array} \right] &= \underbrace{A_5 \rho \sin(u_5) v^2 \left[ \begin{array}{c} -\cos(u_5) \\ \sin(u_5) \\ 0 \end{array} \right]}_{\dot{p}_{out}} - \underbrace{A_5 \rho \sin(u_5) v^2 \left[ \begin{array}{c} -1 \\ 0 \\ 0 \end{array} \right]}_{\dot{p}_{in}} \\ &= A_5 \rho \sin(u_5) v^2 \left[ \begin{array}{c} 1 - \cos(u_5) \\ \sin(u_5) \\ 0 \end{array} \right] \approx A_5 \rho u_5 v^2 \left[ \begin{array}{c} 0 \\ u_5 \\ 0 \end{array} \right] = A_5 \rho u_5^2 v^2 \left[ \begin{array}{c} 0 \\ 1 \\ 0 \end{array} \right] \end{aligned} \quad (8)$$

**Elevator** We can do the same analysis that we did for the rudder with the elevator, which is basically just a rudder that was rotated by 90 degrees. We therefore can approximate the force caused by the elevator as seen in equation 9.

$$\begin{aligned} \left[ \begin{array}{c} F_x \\ F_y \\ F_z \end{array} \right] &= \underbrace{A_4 \rho \sin(u_4) v^2 \left[ \begin{array}{c} -\cos(u_4) \\ 0 \\ \sin(u_4) \end{array} \right]}_{\dot{p}_{out}} - \underbrace{A_4 \rho \sin(u_4) v^2 \left[ \begin{array}{c} -1 \\ 0 \\ 0 \end{array} \right]}_{\dot{p}_{in}} \\ &= A_4 \rho \sin(u_4) v^2 \left[ \begin{array}{c} \cos(u_4) - 1 \\ 0 \\ \sin(u_4) \end{array} \right] \approx A_4 \rho u_4 v^2 \left[ \begin{array}{c} 0 \\ 0 \\ u_4 \end{array} \right] = A_4 \rho u_4^2 v^2 \left[ \begin{array}{c} 0 \\ 0 \\ 1 \end{array} \right] \end{aligned} \quad (9)$$

**Ailerons** The ailerons are modeled the same as the elevator. The forces caused by the left and the right aileron, can be seen in equation 10.

$$\left[ \begin{array}{c} F_x \\ F_y \\ F_z \end{array} \right] \approx A_2 \rho u_2^2 v^2 \left[ \begin{array}{c} 0 \\ 0 \\ 1 \end{array} \right] \quad \left[ \begin{array}{c} F_x \\ F_y \\ F_z \end{array} \right] \approx A_3 \rho u_3^2 v^2 \left[ \begin{array}{c} 0 \\ 0 \\ 1 \end{array} \right] \quad (10)$$

**Propeller** The relation between the control input  $u_1$  and the thrust of the propeller is found experimentally. By attaching the plane to a force gauge with a tether and then actuating the propeller, we can observe force measurements for different thrust inputs. A quadratic function is used to fit a curve into the datapoints. The found relation can be seen in figure 8 and in equation 11.

$$F_{prop}(u_1) = 14.456 \cdot u_1^2 \left[ \begin{array}{c} 1 \\ 0 \\ 0 \end{array} \right] \quad (11)$$

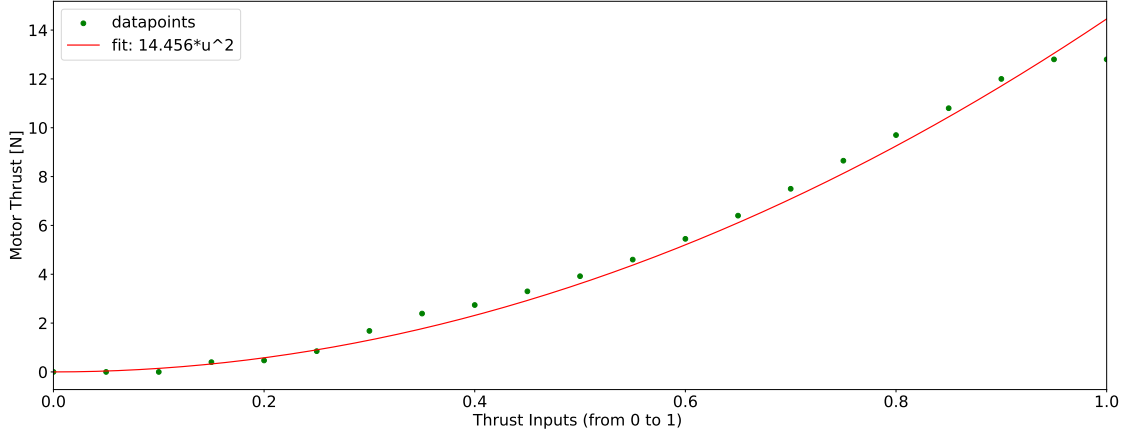


Figure 8: Experimental data points with a quadratic fit.

**Overall Lift and Drag** Finally, we need to determine the lift and drag caused by the airplane regardless of the inputs. We model the plane as an airfoil. According to wing theory by Durand (1935), an airfoil will cause drag and lift according to the relation seen in equation 12. The lift and drag coefficients are dependend on the angle of attack of the plane. These coefficients need to be determined during flight experiments. By analyzing recorded flight data, an expression for  $C_L(\alpha)$  and  $C_D(\alpha)$  can be found.  $A_{tot}$  denotes the area of the airfoil. If it is not determined accurately, the experimental lift and drag coefficients can compensate for it.

$$\begin{aligned} F_{Lift} &= \frac{1}{2} \rho v^2 A_{tot} C_L(\alpha) \\ F_{Drag} &= \frac{1}{2} \rho v^2 A_{tot} C_D(\alpha) \end{aligned} \quad (12)$$

All the forces can be combined to one force and one torque acting on the Center of Mass of the plane. The torques are found by taking the cross product between the forces and the vector from the center of mass to the point of application of the force. A summary of all the forces can be seen in equation 13, where the variables  $d_i$  denote the lever arm for the respective forces.

$$\begin{aligned} F_x &= 14.456 \cdot u_1^2 - \frac{1}{2} \rho v^2 A_{tot} C_D(\alpha) - g \sin(\alpha) \\ F_y &= A_5 \rho u_5^2 v^2 + g \sin(\phi) \cos(\alpha) \\ F_z &= \rho v^2 (A_2 u_2^2 + A_3 u_3^2 + A_4 u_4^2) - g \cos(\phi) \cos(\alpha) + \frac{1}{2} \rho v^2 A_{tot} C_L(\alpha) \\ M_x &= \rho v^2 (A_2 u_2^2 d_2 - A_3 u_3^2 d_3) \\ M_y &= \rho v^2 (A_4 u_4^2 d_4 - A_2 u_2^2 d_2 - A_3 u_3^2 d_3) \\ M_z &= \rho v^2 A_5 u_5^2 d_5 \end{aligned} \quad (13)$$

### 3.3.6 Control Approach

We want to design a controller that can fly a desired trajectory as described in section 3.2 and can perform the agile grapsing maneuver. To achieve this, I propose to split the control task into two different sequences. During the normal flight, we use the standard controller that is already implemented on the Pixhawk. When the object comes closer, the control mode is switched to the 2 Dimensional MPC controller that does a coordinated grasp-flight maneuver to achieve an agile eagle-like pickup. The MPC controller is discussed in section 3.3.7. Figure 9 shows how the controller should switch modes.

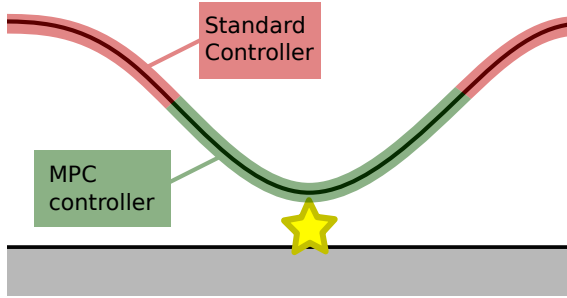


Figure 9: The controller switches modes according to the task that it has to accomplish.

### 3.3.7 Model Predictive Plane Controller

Due to the translational speeds required for flying, the pick-up of the object will be quite challenging. To coordinate the flight behavior with the gripper control, everything should be actuated by the same controller. To make explanations easier, we assume that the pickup happens in the xz-plane and the y coordinate stays constant. With a change in variables, this formulation can be used for a pick-up along an arbitrary direction. The model predictive control approach is discussed in the following steps:

**2D Reduction** We want to achieve the task in the most simple and reliable way, therefore the MPC-problem is reduced to a 2D-problem in the pick-up plane. We use a PID controller to keep the aircraft in the pick-up plane, by controlling the yaw and roll to 0 and the y-coordinate to the object's y-coordinate. This results in the simplifications seen in equation 14.

$$\begin{aligned} \phi = \psi = \dot{\psi} = \dot{\phi} &= 0 \\ y &= y_{obj} \\ u_4 >> u_2, u_3 \rightarrow u_2 &= u_3 = 0 \end{aligned} \tag{14}$$

**State Space and Inputs** After reducing the problem to the 2D case, we end up with the state space variables and inputs seen in table 3.

State Space Variable	Description	Input Variable	Description
$x$	x-Coordinate	$u_1$	Motor Thrust
$z$	z-Coordinate	$u_4$	Elevator
$\alpha$	Plane Pitch	$u_{arm}$	Gripper Arm Torque
$\beta$	Gripper Arm Angle	$u_{grip}$	Gripper Open/Close

Table 3: state space variables and inputs of the MPC-Problem.

**Constraints** The following constraints have to be satisfied by the optimizer:

- C1**  $v_{plane} > v_{stall}$  The plane needs to keep a certain speed to ensure that it has enough lift. The value of  $v_{stall}$  can be determined, by equating the lift with gravity.
- C2**  $\mathbf{u}(t) \in \mathbb{U}$  The control inputs can only be as big as the physical system allow it to be. This means that servos and motors are limited in their range which needs to be taken into account.
- C3**  $\mathbf{x}(t) \in \mathbb{X}$  The state space variables need to stay in a physically allowed range. For example, the gripper angle cannot take a value where the gripper would penetrate the aircraft. Also, the z-coordinate should not be negative and the pitch should stay in a reasonable range.
- C4**  $\mathbf{x}(t_0), \mathbf{x}(t_f)$  Final and initial condition have to be chosen, such that the standard controller can continue the flight after the pickup.

**System Dynamics** The whole system dynamics have been discussed in the sections 3.3.2 and 3.3.5. The reduced system dynamics are summed up in equation 15. These equations will be used to predict the systems behavior in the model predictive controller.  $\mathbf{y}$  denotes a set of convenient variables that are useful to penalize in the cost function. It contains the distance between the aircraft and the pick-up spot in the z-dimension and the speed of the gripper. Both are multiplied by the factor  $(d_{pickup} - |x - x_{obj}|)$  which makes the value bigger, when the x-distance between the plane the object decreases. The variable  $d_{pickup}$  denotes the length of the pick-up phase. With this factor, I hope to maximize the influence on the cost function of these values at the exact moment of pick-up.

$$\frac{d^2}{dt^2} \mathbf{x} = \frac{d^2}{dt^2} \begin{bmatrix} x \\ z \\ \alpha \\ \beta \end{bmatrix} = \begin{bmatrix} -\frac{1}{2 \cdot m} \rho v^2 A_{tot} C_D(\alpha) - \frac{g}{m} \sin(\alpha) \\ \frac{1}{2 \cdot m} \rho v^2 A_{tot} C_L(\alpha) - \frac{g}{m} \cos(\alpha) \\ 0 \\ \frac{\cos(\beta) \cdot g}{m_{gripper} \cdot l_{arm}} \end{bmatrix} + \begin{bmatrix} \frac{14.456 \cdot u_1^2}{\rho v^2 A_4 u_4^2} \\ \frac{m}{\rho v^2 A_4 u_4^2} \\ \frac{\rho v^2 A_4 u_4^2 d_4}{m_{gripper} l_{arm}} \\ \frac{I_{pitch}}{u_{arm}^2} \\ \frac{I_{pitch}}{m_{gripper} l_{arm}^2} \end{bmatrix} \quad (15)$$

$$\mathbf{y} = \begin{bmatrix} y_z \\ y_{grip} \end{bmatrix} = \begin{bmatrix} \Delta z \\ \frac{(z - z_{obj} + d_{arm}) \cdot (d_{pickup} - |x - x_{obj}|)}{|\vec{x} + \dot{\beta} \times \vec{r}_{plane-grip}| \cdot (d_{pickup} - |x - x_{obj}|)} \\ \text{gripper speed} \end{bmatrix}$$

**Nonlinear Quadratic Optimal Control** The nonlinear system dynamics are discretized and brought into a form seen in equation 16.

$$\begin{aligned} \mathbf{x}_{n+1} &= f_d(\mathbf{x}_n, \mathbf{u}_n) \\ \mathbf{y}_n &= g_d(\mathbf{x}_n) \end{aligned} \quad (16)$$

With that we can formulate the quadratic cost function seen in equation 17, where  $\mathbf{P}, \mathbf{Q}$  and  $\mathbf{R}$  are weight matrices for the different variables. In an iterative manner, the optimal weights are found, which should result in the desired pick-up discussed in section 3.1. I expect, that a penalization of the gripper speed will cause the plane to slow down close to  $v_{stall}$  and swing the arm in the contrary direction of flight. It is very likely, that during the development of the MPC, new problems will arise which will require some modification of the proposed approach.

$$\mathbf{J}(\mathbf{x}_k, \mathbf{u}_k) = \mathbf{x}_{k+N}^\top \mathbf{P} \mathbf{x}_{k+N} + \sum_{i=0}^{N-1} (\mathbf{y}_{k+i}^\top \mathbf{Q} \mathbf{y}_{k+i} + \mathbf{u}_{k+i}^\top \mathbf{R} \mathbf{u}_{k+i}) \quad (17)$$

As seen in equation 18, the optimal control inputs are found by optimizing over the cost function  $\mathbf{J}$ .

$$\mathbf{U}_k^*(x_k) := \arg \min_{\mathbf{U}_k} \mathbf{J}(\mathbf{x}_k, \mathbf{U}_k) \quad (18)$$

### 3.4 Controller Architecture

The MPC runs on the Raspberry Pi and gives control inputs to the plane over the Pixhawk. It can also actuate the gripper through the Arduino. An extended kalman filter (EKF) is used for state estimation. It runs on the Pixhawk, because the firmware has great ready-to-use implementation. To function properly the EKF needs sensor information from both the real time kinematic positioning system (RTK GPS) as well as the inertial measurement unit (IMU). A schematic view of the control architecture can be seen in figure 10. The Arduino is needed to actuate the gripper, because the Raspberry Pi is not suited to directly actuate the motors and servos in the gripper. If I discover a way to actuate the gripper and the arm without an Arduino during the development of the system, I will remove the Arduino from the system architecture.

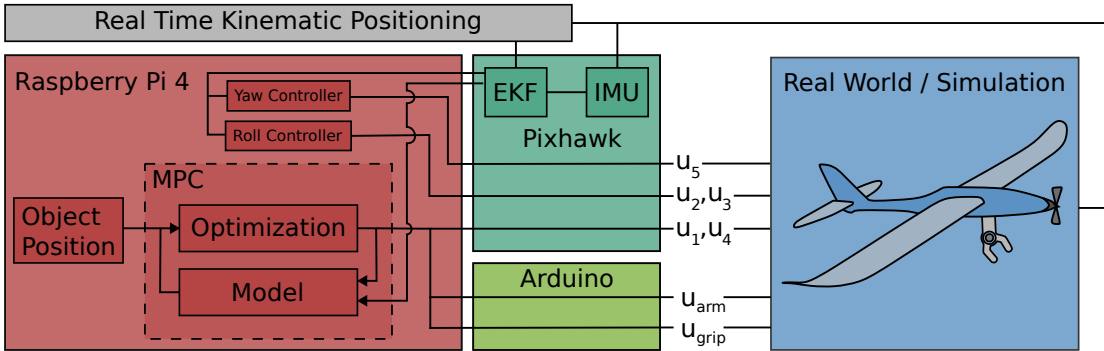


Figure 10: The proposed control architecture with a MPC-controller running on the companion computer and a EKF running on the Pixhawk. The components on the Pixhawk are already implemented, whereas the elements on the Raspberry are newly developed.

### 3.5 System Architecture

The system architecture is inspired by the work of Appius et al. (2022), who used a similar approach for dynamic grasping of objects with quadcopters. The following list should clarify the components function and interconnections. A schematic view of the system architecture can be seen in figure 11.

**Real Time Kinematic Positioning (RTK GPS)** is used for determining the position of the aircraft. The system works by comparing the GPS signal of a fixed ground station with the GPS signal on the aircraft. With this, centimeter level accuracy can be achieved at a frequency of 20 Hertz. This is enough to accurately control the aircraft's position in a pick-up task. It works out-of-the-box with the Pixhawk flight controller.

**Arduino** The Arduino is used to actuate the gripper. It communicates with the Raspberry Pi over a serial connection. The arduino is needed, because it is impractical and inaccurate to directly actuate motors from the Raspberry's GPIO pins.

**Raspberry Pi** The Raspberry Pi is used as a companion computer for the flight controller. It runs the MPC Controller and sends motor commands to the flight controller. It reads state information from the Flight controller's EKF.

**Pixhawk** The Pixhawk is the flight controller. It is used to make the actuation of the motors easier and to get state estimation from the built-in EKF, which uses information from the IMU and RTK GPS. The raspberry and the pixhawk communicate over serial connection.

**Ground Computer** The ground computer is used as an interface for the user. High-level commands are sent to the raspberry over an SSH session. The ground computer and raspberry communicate over SiK radio.

**RC Remote** The radio control remote is used as a secondary communication channel, which can be used for testing or emergency situations. It does not communicate over the raspberry pi but directly with the Pixhawk flight controller.

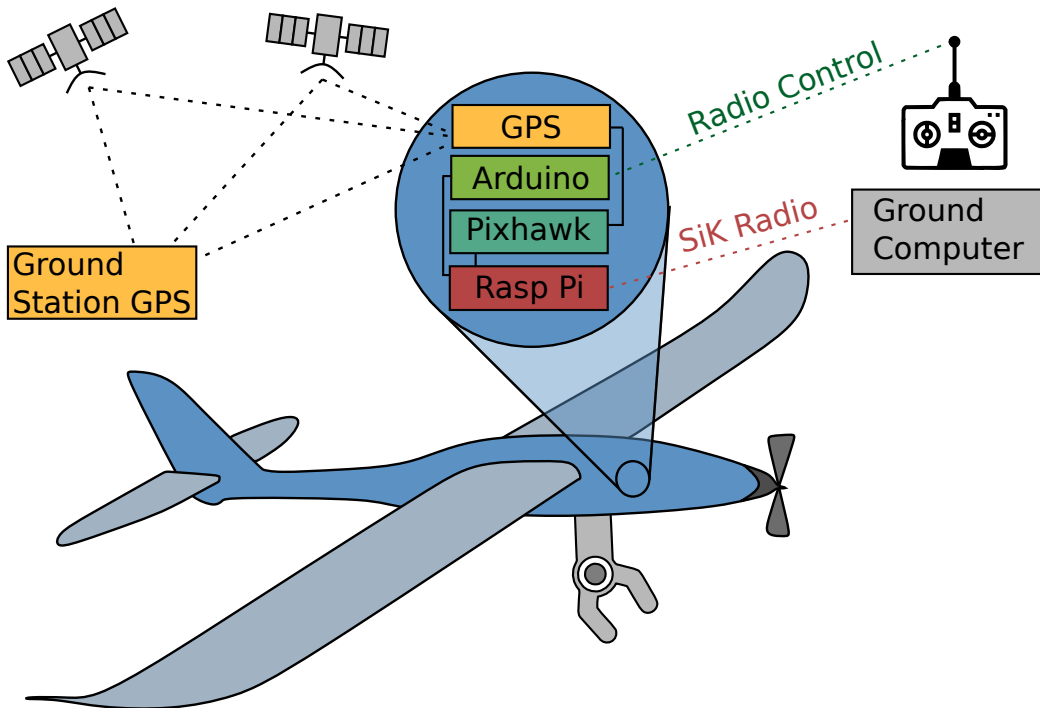


Figure 11: A schematic view of system architecture with all its components and connections

### 3.6 Timeline

An approximate timeline of the thesis can be seen in the Gantt chart in figure 12.

## 4 Future Work

Future work would be to not only grasp objects that lie still on the ground, but also moving objects or even flying ones. The control framework proposed in this thesis would still be useful, but some changes in the trajectory generation would probably be necessary. Another further improvement would be to capture objects, without placing them at a predefined position. To achieve this, a perception algorithm to detect the object would be needed. A way for the system to dodge objects like trees or houses would also be an important future workpackage. This could be done by using a self localization and mapping package (SLAM) that could use event cameras.

In this thesis we neglected the influence of winds. The robot will only pick-up objects in wind-still conditions. In case of stronger winds, the controller would need to be updated to compensate for side, back and front winds during both flight and pickup.

To go even further towards nature, the plane architecture could be replaced with a bird-like ornithopter. This is an aircraft that flies by flapping its wings. A grasp could probably be made even more energy efficient and fast when working with such an aircraft.

All in all, there is still a lot of work to do when it comes to bio inspired grasping. Real-world fully alive eagles are still miles ahead when compared to the most modern grasping robots.

## References

- Appius, A. X., Bauer, E., Blochlinger, M., Kalra, A., Oberson, R., Raayatsanati, A., Strauch, P., Suresh, S., von Salis, M., & Katzschmann, R. K. (2022). Raptor: Rapid aerial pickup and transport of objects by robots. *ArXiv, abs/2203.03018* (cit. on pp. 1, 11).

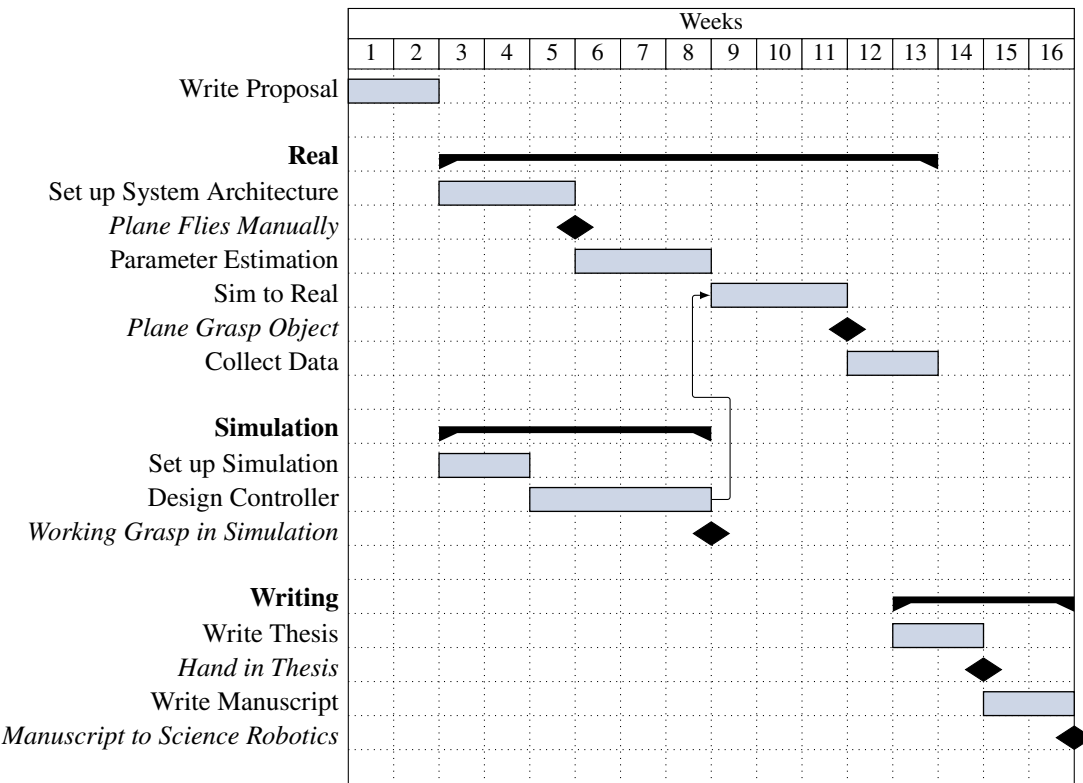


Figure 12: Gantt Chart

- Durand, W. F. (1935). Basic ideas of wing theory: Flow around an airfoil. In W. F. Durand (Ed.), *Aerodynamic theory: A general review of progress under a grant of the guggenheim fund for the promotion of aeronautics* (pp. 1–24). Springer Berlin Heidelberg. [https://doi.org/10.1007/978-3-642-91485-0\\_1](https://doi.org/10.1007/978-3-642-91485-0_1). (Cit. on p. 8)
- Fiaz, U. A., Abdelkader, M., & Shamma, J. S. (2018). An intelligent gripper design for autonomous aerial transport with passive magnetic grasping and dual-impulsive release. *2018 IEEE/ASME International Conference on Advanced Intelligent Mechatronics (AIM)*, 1027–1032 (cit. on p. 1).
- Fishman, J., Ubellacker, S., Hughes, N., & Carbone, L. (2021). Dynamic grasping with a "soft" drone: From theory to practice. *2021 IEEE/RSJ International Conference on Intelligent Robots and Systems (IROS)*, 4214–4221 (cit. on p. 1).
- Gawel, A., Kamel, M., Novkovic, T., Widauer, J., Schindler, D., von Altishofen, B. P., Siegwart, R. Y., & Nieto, J. I. (2017). Aerial picking and delivery of magnetic objects with mavs. *2017 IEEE International Conference on Robotics and Automation (ICRA)*, 5746–5752 (cit. on p. 1).
- Hingston, L., Mace, J., Buzzatto, J., & Liarokapis, M. (2020). Reconfigurable, adaptive, lightweight grasping mechanisms for aerial robotic platforms. *2020 IEEE International Symposium on Safety, Security, and Rescue Robotics (SSRR)*, 169–175 (cit. on p. 1).
- Karydis, K., & Kumar, V. R. (2017). Energetics in robotic flight at small scales. *Interface Focus*, 7 (cit. on p. 1).
- Koken, M. (2017). The experimental determination of the moment of inertia of a model airplane (cit. on p. 5).
- McLaren, A. I., Fitzgerald, Z., Gao, G., & Liarokapis, M. (2019). A passive closing, tendon driven, adaptive robot hand for ultra-fast, aerial grasping and perching. *2019 IEEE/RSJ International Conference on Intelligent Robots and Systems (IROS)*, 5602–5607 (cit. on p. 1).
- Meng, J., Buzzatto, J., Liu, Y., & Liarokapis, M. (2021). On aerial robots with grasping and perching capabilities: A comprehensive review. *Frontiers in Robotics and AI*, 8 (cit. on pp. 1, 2).
- New York Post. (2017). *Bald eagle snatches salmon right off fisherman's boat*. Retrieved October 3, 2022, from <https://nypost.com/video/bald-eagle-snatches-fishermans-salmon-right-off-his-boat/>. (Cit. on p. 1)

- 
- Noth, A., Bouabdallah, S., & Siegwart, R. Y. (2006). Dynamic modeling of fixed-wing uavs (cit. on p. 4).
- Roderick, W. R. T., Cutkosky, M. R., & Lentink, D. (2021). Bird-inspired dynamic grasping and perching in arboreal environments. *Science Robotics*, 6 (cit. on p. 1).
- Stewart, W., Ajanic, E., Muller, M., & Floreano, D. (2022). How to swoop and grasp like a bird with a passive claw for a high-speed grasping. *IEEE/ASME Transactions on Mechatronics* (cit. on p. 1).
- Thomas, J. R., Loianno, G., Polin, J., Sreenath, K., & Kumar, V. R. (2014). Toward autonomous avian-inspired grasping for micro aerial vehicles. *Bioinspiration & Biomimetics*, 9 (cit. on p. 1).
- Zhang, H., Sun, J., & Zhao, J. (2019). Compliant bistable gripper for aerial perching and grasping. *2019 International Conference on Robotics and Automation (ICRA)*, 1248–1253 (cit. on p. 1).
- Zhu, Y., Guo, Q., Tang, Y., Zhu, X., He, Y., Huang, H., & Luo, S. (2022). Cfd simulation and measurement of the downwash airflow of a quadrotor plant protection uav during operation. *Computers and Electronics in Agriculture* (cit. on p. 1).



Eidgenössische Technische Hochschule Zürich  
Swiss Federal Institute of Technology Zurich

**Title of work:**

Development of a Model Predictive Controller for FALCON:  
Fixed-wing Aerial Lifting and Carrying of Objects inspired  
by Nature

**Thesis type:**

Semester Project Proposal

**Student:**

Name: Aurel X. Appius  
E-mail: appiusa@ethz.ch  
Student ID: 19-916-204

**Supervisors:**

Yasunori Toshimitsu  
Prof. Dr. Robert K. Katzschatmann

**Declaration of originality**

I hereby confirm that I am the sole author of the written work here enclosed and that I have compiled it in my own words. Parts excepted are corrections of form and content by the supervisor.

With my signature I confirm that

- I have committed none of the forms of plagiarism described in the '[Citation etiquette](#)' information sheet.
- I have documented all methods, data and processes truthfully.
- I have not manipulated any data.
- I have mentioned all persons who were significant facilitators of the work.

I am aware that the work may be screened electronically for plagiarism.

**Signature:**

Zürich, October 20, 2022